

# A NONLINEAR VISCOELASTIC MODEL FOR ELECTROACTIVE INFLATED MEMBRANES

Stefano Buoso\* and Rafael Palacios\*

\* Department of Aeronautics  
Imperial College London  
London SW7 2AZ, United Kingdom  
e-mail: s.buoso12@imperial.ac.uk

**Key words:** Dielectric Elastomers, Hyperelastic, Inflated Membrane, Tunable Lens, Viscoelasticity

**Abstract.** Predictive materials models for dielectric elastomers are required to assess their performance in complex applications and improve those designs. The main challenge is the characterisation of the large deformations typical of their applications and by the rate dependent constitutive law. This work proposes a nonlinear-viscoelastic material model for the VHB4905 polymer suitable for implementation in a general-purpose finite-element code. The elastic part has been proven to predict the performance of different devices considered. The viscoelastic part of the constitutive model has been fitted with experimental data available in the literature and also showed a good agreement with the case considered.

## 1 Introduction

Dielectric elastomers (DEs) are being considered in a new generation of smart devices. Heart pumps and cardiac valves [1], artificial muscles [2], tunable lenses [3, 4] and membrane wings [5], just to name a few of them, can be redesigned to embed these materials. The absence of mechanisms and the simplicity of construction could reduce the weight and the cost of the devices and increase their reliability. In the biomedical field, Tews et al. [1] measured the pressure-volume characteristics of dielectric elastomer diaphragms to investigate the use of DEs for cardiac applications. Tunable lenses made with dielectric elastomers have been studied in Refs. [3, 4]. Hochradel et al.[6] proposed an acoustic device made with an acrylic elastomer, VHB4905. All the aforementioned studied, except for [6], were focused on the static characterisation of the material performances, neglecting the visco-elastic time dependent behaviour that is fundamental when dynamic applications are considered. To reproduce these experiments and predict the behaviour of DEs an electromechanical constitutive model able to deal with large deformations, material

nonlinearities, viscoelastic effects, and electrostriction [7].

Experimental characterisation tests have often been too simplistic compared to actual loading conditions in typical applications. Typical examples can be found in [8, 9] where uniaxial tests are considered representative of the general behaviour of DEs. This is one of the factors that have led to a poor matching between experiments and numerical simulations. and has been presented also by [10], who showed how passing from uniaxial to equi-biaxial loading conditions requires the coefficients of the material model to be modified.

Another limitation of the majority of existing models is that viscoelastic effects are either neglected or modelled with a linear approach [9]. Wissler and Mazza [9] proposed a linear viscoelastic approach based on Prony series to model the viscoelastic behaviour of the material. However, the agreement between the model and experimental results indicates that a viscoelastic linear approach is not appropriate for DE with large strains. Alternatively, Mokarram et al. [11] used the multiplicative decomposition approach to model the viscoelastic behaviour of DE for a tensile test. The results showed a good agreement for a wide range of deformation velocities, both for loading and unloading conditions.

This work proposes a dynamic, non-linear visco-hyperelastic model coupled with a linear electric model suitable for finite-element software implementation. It is based on a non-linear viscous model with a linear evolution law [12]. The implementation of the model has been verified against experimental uniaxial data [11], showing a very good agreement. Numerical simulations involving loads similar to the conditions encountered in aeronautical and biological applications, i.e. membrane inflation, are compared with dynamic experiments available in literature. The same model is also used to evaluate the static performance of tunable lenses made with dielectric elastomer actuators. The aim is to reproduce recent experimental results [4] in which the lenses are made of two transparent prestretched circular DE enclosing a fluid volume and demonstrate that the model proposed is predictive of the performances of an actual device.

## 2 Constitutive Model

### 2.1 Assumptions

An isotropic constitutive model will be assumed. This has been experimentally verified up to a stretch of 1.5 [13], but would need further investigation for higher stretches. The electrostatic stresses are decoupled from the mechanical ones, such that the total stress tensor  $\boldsymbol{\sigma}$  is [7]

$$\boldsymbol{\sigma} = \boldsymbol{\sigma}_m + \boldsymbol{\sigma}_{el} \tag{1}$$

where  $\boldsymbol{\sigma}_m$  and  $\boldsymbol{\sigma}_{el}$  are the mechanical and electromechanical stress tensors. In addition to this, the viscoelastic stresses are assumed to be related only to the deviatoric part of the deformation gradient [14]. This will be described in Section 2.2. It is also assumed the independence of the electrostatic stresses from the viscoelastic behaviour of the material, so that they only depend on the purely elastic deformation [7]. The evolution of the

electrostatic forces is further assumed to be instantaneous, since its time scale is several order of magnitude faster than the mechanical ones. The electric model also neglects the electrostrictive (non-linear) effects and a constant value of the dielectric constant is assumed for the range of the deformation in the model proposed [15]. Zhao and Suo [16] showed that when considering a wide range of strains, electrostrictive effects can be not negligible and need to be included in the model.

## 2.2 Mechanical Material Model

The viscoelastic constitutive model for DEs is developed in the finite deformation framework [12, 17, 14]. Consider a body in the reference configuration  $\mathcal{B}_0$ , with  $\mathbf{X}$  the initial position vector identifying each particle in the domain. At time  $t$  the body is in the new, actual configuration  $\mathcal{B}$  and the motion of the particle is tracked by the mapping  $\mathbf{x} = \phi(\mathbf{X}, t)$ . The *deformation gradient*  $\mathbf{F}$  at the time  $t$  is defined as the gradient of  $\phi$  in the reference coordinate system,  $\mathbf{F} = \nabla_{\mathbf{X}}\phi$  where  $\nabla_{\mathbf{X},j} = \frac{\partial}{\partial X_j}$ . The description of the kinematics of the model uses the multiplicative decomposition of  $\mathbf{F}$  into its volumetric and isochoric components, that is, [18]

$$\bar{\mathbf{F}} = \mathbf{F} J^{-\frac{1}{3}} \quad (2)$$

where  $\bar{\mathbf{F}}$  maps the isochoric deformation of the body and  $J = \det(\mathbf{F})$  is related to the change in volume. The volumetric part is assumed to be purely elastic, while the deviatoric contribution is decomposed into the elastic and viscous parts. The viscous contribution is obtained through the multiplicative decomposition of  $\bar{\mathbf{F}}$  into its elastic and viscous components [12]. Considering a number  $N$  of relevant viscous mechanisms involved in the material constitutive model, for each of them, we define a correspondent elastic tensor  $\bar{\mathbf{F}}_{e\alpha}$

$$\bar{\mathbf{F}}_{e\alpha} = \bar{\mathbf{F}} \mathbf{F}_{v\alpha}^{-1} \quad (3)$$

where  $\mathbf{F}_{v\alpha}$  is the viscous tensor associated with the  $\alpha$ -th viscous mechanisms considered.  $\mathbf{F}_{v\alpha}$  represents the internal variables describing the nonequilibrium evolution of the material constitutive law

$$\dot{\mathbf{C}}_{v\alpha} = \frac{1}{\tau_\alpha} [\mathbf{C} - \mathbf{C}_{v\alpha}] \quad (4)$$

which is a linearisation of the one proposed by [17] where  $\tau_\alpha$  is the time constant relative to the  $\alpha$  relaxation mechanisms considered and has to be experimentally determined. By construction, it is  $\det(\mathbf{F}_{v\alpha}) = 1$ . The viscoelastic stresses for each viscous mechanism are expressed as function of  $\bar{\mathbf{F}}_{e\alpha}$ . The evolution of the internal variables from the initial condition considered, is driven by an internal evolution law  $\dot{\bar{\mathbf{F}}}$  and the thermodynamic equilibrium is reached when  $\mathbf{F}_{v\alpha} = \bar{\mathbf{F}}$ . Thus at equilibrium  $\bar{\mathbf{F}}_{e\alpha} = \mathbf{I}$  and hence the elastic stresses are zero. For the general derivation of the evolution law see [12, 17]. In this work a linearised version of the evolution law is considered (Section 2.2), but that model can be easily modified with a different one.

The isotropic assumption allows the definition of the free-energy function of the material in terms of the invariants of the right Cauchy-Green deformation tensors.  $\bar{\mathbf{C}} = \bar{\mathbf{F}}^T \bar{\mathbf{F}}$  is used for the deviatoric elastic contribution and  $\bar{\mathbf{C}}_{e\alpha} = \bar{\mathbf{F}}_{e\alpha}^T \bar{\mathbf{F}}_{e\alpha}$  for the viscous contribution.  $J$  is used for the volumetric contribution [17]. This removes the dependency of the stresses on the material orientation. Thus the free energy function is of the form

$$W = U(J) + \Phi_\infty(\bar{I}_1, \bar{I}_2) + \sum_{\alpha=1}^N \Phi_{v\alpha}(\bar{I}_{1e\alpha}, \bar{I}_{2e\alpha}) \quad (5)$$

where  $U(J)$  is the volumetric energy function accounting for the variation in volume defined by  $J$ ,  $\Phi_\infty(\bar{I}_1, \bar{I}_2)$  is the deviatoric free energy function expressed in terms of  $\bar{I}_1$  and  $\bar{I}_2$ , which are the first and second invariants of  $\bar{\mathbf{F}}$ , respectively

$$\bar{I}_1 = \text{tr} \bar{\mathbf{C}} \quad \bar{I}_2 = \frac{1}{2} \left( (\text{tr} \bar{\mathbf{C}})^2 - \text{tr} \bar{\mathbf{C}}^2 \right) \quad (6)$$

and  $\Phi_{v\alpha}(\bar{I}_{1e\alpha}, \bar{I}_{2e\alpha})$  is the energy function corresponding to the viscoelastic stresses related to the  $\alpha$ -th mechanism.  $\bar{I}_{1e\alpha}$  and  $\bar{I}_{2e\alpha}$  are the first and second invariants of  $\bar{\mathbf{C}}_{e\alpha}$  defined in (3)

$$\bar{I}_{1e\alpha} = \text{tr} \bar{\mathbf{C}}_{e,\alpha} \quad \bar{I}_{2e\alpha} = \frac{1}{2} \left( (\text{tr} \bar{\mathbf{C}}_{e\alpha})^2 - \text{tr} \bar{\mathbf{C}}_{e\alpha}^2 \right) \quad (7)$$

The stresses are derived from the free energy function through the derivation respect to the stretches in the directions considered [17]. In the reference configuration the stresses are

$$\mathbf{S} = 2 \frac{\partial W}{\partial \mathbf{C}} = 2\mathbf{S}_J + 2\mathbf{S}_\infty + 2\mathbf{S}_v = J \frac{\partial U}{\partial J} \mathbf{C}^{-1} + 2J^{-\frac{2}{3}} \mathbb{P} : \left( \frac{\partial \Phi_\infty}{\partial \bar{\mathbf{C}}} + \frac{\partial \Phi_v}{\partial \bar{\mathbf{C}}} \right) \quad (8)$$

where  $\mathbf{S}$  is the second Piola-Kirchhoff stress tensor,  $\mathbf{S}_J$  are the stresses due to the contribution of the volumetric energy function,  $\mathbf{S}_\infty$  is the contribution of the elastic deviatoric stresses,  $\mathbf{S}_v$  the viscous stresses, and the projection tensor is  $\mathbb{P} = \mathbb{I} - \frac{1}{3} \mathbf{C}^{-1} \otimes \mathbf{C}$  with  $\mathbb{I}$  the symmetric fourth-order identity tensor. The stress tensor in the deformed configuration  $\boldsymbol{\sigma}$  is finally obtained through a push-forward operation on  $\mathbf{S}$

$$\boldsymbol{\sigma} = \frac{1}{J} \mathbf{F}^T \mathbf{S} \mathbf{F} \quad (9)$$

In (5) we introduced the free energy function. Several models have been proposed in the literature [8, 9, 10, 19, 20, 21, 22] offering different behaviours of the constitutive model of the material. For any of them the coefficients have to be determined experimentally and usually static uniaxial tests are considered. The issue is that, even if data are obtained for very slow deformation rates, they include some viscoelastic effects. To the best of the authors' knowledge, only [21, 11, 13] obtained static results on DEs including material relaxation.

### 2.2.1 Electrostatic Stresses

The electrostatic stresses are modelled with the Maxwell's stress tensor. Given an electric field vector  $\mathbf{E}$ , the stress tensor  $\boldsymbol{\sigma}_{el}$  is defined as [7]

$$\boldsymbol{\sigma}_{el} = \epsilon \mathbf{E} \otimes \mathbf{E} - \frac{1}{2} \epsilon (\mathbf{E} \cdot \mathbf{E}) \mathbf{I}, \quad (10)$$

where  $\epsilon$  is the material dielectric constant,  $\mathbf{E}$  is the electric field vector in the deformed coordinate system and  $\mathbf{I}$  is the unitary second order tensor.

### 2.2.2 Tangent Stiffness Matrix

To use the constitutive model in a finite-element model that adopts a Newton-Raphson scheme, the tangent stiffness matrix needs to be evaluated to build the operator for the iterative solution scheme. The tangent stiffness matrix  $\mathbb{C}$  in the reference configuration is obtained as [17]

$$\mathbb{C} = 2 \frac{\partial \mathbf{S}}{\partial \mathbf{C}}, \quad (11)$$

and in  $\mathbf{S}$  all the stresses contributions, elastic (volumetric and deviatoric) and viscous (deviatoric) are included. The derivation of the expression of (11) can be found in [23]. The tensor can be written in the deformed coordinate system by means of a push forward operation  $\mathbb{C}_{ijkl}^a = F_{ip} F_{jq} F_{kr} F_{ls} \mathbb{C}_{pqrs}$

## 3 Inflated membrane model

The previous model will be used in this work to study the behaviour of inflatable circular DE. We will consider an axial-symmetric simplified model assuming spherical deformation of the inflated membrane. This assumption is representative of the real behaviour of an inflated circular membrane when the ratio between the maximum camber amplitude and the initial diameter is below 15% [4].

### 3.1 Analytical membrane model

Consider a prestretched circular membrane with initial diameter  $2a$  and radial pre-stretch  $\lambda_p$ . The initial thickness is  $H$  and, assuming incompressibility, the thickness of the stretched membrane is  $h = H\lambda_p^{-2}$ . If  $z$  is the out-of-plane displacement of the centre of the membrane, the radius  $R$  of the correspondent spherical cap is related to  $z$  by

$$z = R - \sqrt{R^2 - a^2} \quad (12)$$

Considering Newton's second law of dynamics for a membrane element of infinitesimal area subjected to a uniform pressure difference  $\Delta P$  and uniform tension  $T$ , we obtain

$$\rho h \frac{\partial^2 z}{\partial t^2} = -\frac{2T}{R} + \Delta P \quad (13)$$

where  $\rho$  is the membrane density,  $t$  is the membrane thickness and  $T$  is the in-plane tension per unit of area of the membrane. In the case of actuated DE,  $T$  is the sum of the mechanical elastic and viscoelastic in-plane stresses and the equivalent in-plane Maxwell stress for incompressible materials,  $-\epsilon E^2$  [7]. If we consider the static equilibrium, the displacement  $z$  due to  $\Delta P$  is given by

$$\Delta P = 2T \left( \frac{1}{R} \right) \quad (14)$$

where  $T$  in this case is the sum of the purely elastic stresses and the Maxwell stress. Combining (12) and (14) we have

$$z = \frac{2T}{\Delta P} - \sqrt{\left( \frac{2T}{\Delta P} \right)^2 - a^2}. \quad (15)$$

For low values of  $z$ ,  $T$  can be assumed as a constant in the problem. When the deformation increases the tension needs to be recomputed considering the updated value of the stretch due to the out-of-plane displacement. For a given the displacement  $z$ , the updated membrane length  $L$  is

$$L = \lambda_p \arcsin \left( \frac{a}{R} \right) R \quad (16)$$

which can be used in the material model (5) to compute the new in-plane tension  $T$  and an updated value of  $z$  till convergence.

Consider now a reference static configuration identified by the parameters  $\Delta P_0$ ,  $T_0$ ,  $z_0$  and  $R_0$ . Consider now a perturbation of the static equilibrium that can be due to a variation of the actuation voltage that causes a variation of the Maxwell stress  $\delta\sigma_{el}$ , or a fluctuation of the difference of pressure  $\delta P$ . Expanding (13) from the reference configuration and linearising we have

$$\rho h \frac{\partial^2 z}{\partial t^2} = -\frac{2\delta T}{R_0} + \frac{2T_0}{R_0^2} \delta R + \delta P \quad (17)$$

where  $\delta T$  is the variation of in-plane tension considering the elastic, viscous and Maxwell contributions and  $\delta R$  is the variation of  $R$  due to  $z$ . It is possible to express  $\delta T$  as function of  $z$  and  $\delta\sigma_{el}$ . however, the variation of the elastic tension due to the deformation, in the range of validity of this linearised model, is negligible. Thus  $\delta T$  is written as the sum of the contribution of the viscoelastic stresses and the Maxwell stresses. Using the Laplace transform for (17)

$$\rho h s^2 \mathcal{L}\{z\} = -\frac{2\mathcal{L}\{\delta T\}}{R_0} + \frac{2T_0}{R_0^2} \mathcal{L}\{\delta R\} + \mathcal{L}\{\delta P\} \quad (18)$$

Through linearisation  $\delta R$  can be expressed as

$$\delta R = \frac{z_0^2 - a^2}{2z_0} z \quad (19)$$

Considering a linearised form of the viscoelastic stresses,  $\mathcal{L}\{\delta T\}$  can be written as

$$\mathcal{L}\{\delta T\} = \mathcal{L}\{\delta\sigma_{el}\} + \sum_{\alpha=1}^N \Omega(\mathbf{x}_\alpha, s) \Gamma \mathcal{L}\{z\} \quad (20)$$

where  $N$  is the number of viscoelastic mechanisms considered,  $\Gamma = \Gamma(a, h_0, R_0)$  is a function of the initial conditions to linearise the variation of the length of the spherical cap and  $\Omega(\mathbf{x}_\alpha, s)$  is the transfer function from the membrane stretch ( $\Gamma \mathcal{L}\{z\}$ ) to the viscous stresses.

Substituting (20) and the Laplace transform of (19) in (18) the linear dynamics of the system is

$$\mathcal{L}\{z\} = \frac{2\mathcal{L}\{\delta\sigma_{el}\} R_0^{-1} + \mathcal{L}\{\delta P\}}{\rho h s^2 + \sum_{\alpha=1}^N \Omega(\mathbf{x}_\alpha, s) \Gamma - \frac{2T_0}{R_0^2} \frac{z_0^2 - a^2}{2z_0}} \quad (21)$$

Equation (21) represents the linear response of the inflated membrane when a variation in pressure or voltage is applied over the reference configuration considered.

When a mechanical constitutive model  $W$  is selected, the mechanical stresses can be computed. The elastic tension  $T_0$  is equal to  $\sigma_0 H \lambda_p^2$  where  $\sigma_0$  is the in-plane tension obtained from

$$\boldsymbol{\sigma} = \left( -p \mathbf{I} + 2 \frac{\partial \Phi_\infty}{\partial I_1} \mathbf{C} \right) \quad (22)$$

where  $\mathbf{C}$  is the left Cauchy Green deformation gradient and  $p$  is the hydrostatic pressure that is determined from the plane stress condition on the membrane,  $\sigma_0^{(3,3)} = 0$ . The Maxwell stress, using the incompressibility assumption, is

$$\sigma_{el} = -\epsilon \left( \frac{V}{H} \lambda_p^2 \right)^2 H \lambda_p^{-2} \quad (23)$$

where  $V$  is the applied voltage. The viscoelastic model proposed in Section 2.2 is linearised and coupled with the evolution law giving the following expression of  $\Omega(\mathbf{x}_\alpha, s)$  for (20)

$$\Omega(\mathbf{x}_\alpha, s) = \frac{\mu_\alpha s}{\frac{1}{\tau_\alpha} + s} \quad (24)$$

This is the linear transfer function of the Maxwell elastic element.

### 3.2 Viscoelastic Material Model for VHB4905

A second, detailed, model is proposed next as a material model to simulate an actuated inflated membrane made of VHB4905 based on the formulation defined in Section 2. First, static and dynamic results available from [8, 21] will be used to define the coefficients of the material model. From [21], the initial membrane thickness is 0.5 mm, the final radius

is 88.9 mm with a prestretch of 3.5 [21]. The elastic constitutive law considered is the Gent incompressible model [24]

$$\Phi_\infty = -\frac{\mu J_m}{2} \log \left( 1 - \frac{I_1 - 3}{J_m} \right) \quad (25)$$

where  $\mu$  is the shear modulus of the material and  $J_m$  is a coefficient related to the limiting stretching value of the polymer. The viscoelastic energy function selected for the different mechanism is the incompressible Neo-Hookean model

$$\Phi_{v,\alpha} = \frac{\mu}{2} (\bar{I}_{e1,\alpha} - 3) \quad (26)$$

with a linear evolution law (4).

### 3.2.1 Definition of $\Phi_\infty$

The first step in the definition of the material model is the determination of the coefficients of  $\Phi_\infty$ , in this case the values of  $\mu$  and  $J_m$  for the Gent model selected. The static model (15) with the iterative correction of the tension (16) has been used to define a least-square fitting process with the static data in [21] to identify the best value of the coefficients. The coefficients obtained were found to be close to  $\mu=20\text{kPa}$ ,  $J_m=100$  and  $\epsilon_r=2.7$  and those are the values that will be used for the model. The coefficients are used to reproduce the membrane inflation with three different models: The analytical models proposed in this section (linear and nonlinear) and a model defined using a commercial finite element software are considered. The results are presented in Fig. 1 and compared with the experimental data. It can be seen that the range of validity of the linear model is limited and is overestimating the deformed configuration since the elastic tension is not updated. The nonlinear model is in very good agreement with both the experiments and the finite element model.

### 3.2.2 Definition of $\Phi_{v,\alpha}$

The model is based on the fitting of the actuated membrane experiments proposed in Ref. [21]. The circular membrane is inflated with a bias pressure of 80 Pa and actuated with a sinusoidal voltage with amplitude,  $\Phi$ , of 1.5 kV and various frequencies. The Maxwell stress is

$$\sigma_{el} = -\epsilon \left( \frac{\Phi}{H} \lambda_p^2 \right)^2 \sin^2(2\pi\nu t) = -\epsilon \left( \frac{\Phi}{H} \lambda_p^2 \right)^2 \frac{1 - \cos(2\pi\nu t)}{2} \quad (27)$$

The reference configuration selected for the membrane is represented by the static equilibrium with  $\Delta P_0 = 80$  Pa and a constant Maxwell stress equal to the mean value in (27),  $-\frac{\epsilon}{2} \left( \frac{\Phi}{H} \lambda_p^2 \right)^2$ . With this reference condition, using (18), the transfer function of

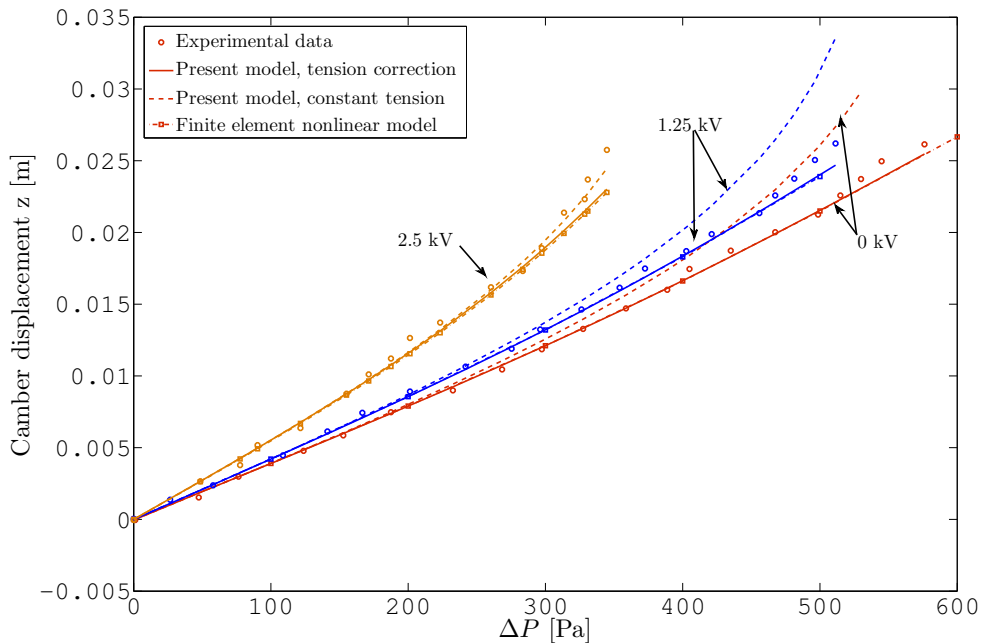


Figure 1: Static fitting of an inflated membrane of VHB4905 for 0 kV (red), 1.25 kV (blue) and 2.5 kV (orange) of applied voltage. Symbols represent experimental data from [21] and continuous lines the predictions of the numerical models proposed.

the membrane is defined. The expressions of the amplitude and phase delay of the forced response are used in a least-square fitting problem in order to identify the viscoelastic coefficients of the viscoelastic model. Only one viscoelastic mechanism has been considered, representing a good compromise between computational cost and accuracy of the results. The coefficients are  $\mu_\alpha = 32.27$  MPa and  $\tau_\alpha = 2.01 \cdot 10^{-4}$  s.

The results are plotted against the experimental data from [8, 21] in Fig. 2 in two different conditions showing a good agreement. The first natural frequency of the membrane, including the viscoelastic effects, is found to be 69 Hz, which is close to the 70 Hz reported in the experiments [21].

#### 4 Tunable Lens Model

The material model for VHB4905 proposed in Section 3.2 is used to reproduce the experimental results of [4] on a tunable lens. The lens is composed of two membranes made of transparent DE membranes and mounted on a rigid frame (Fig.3a). A transparent fluid is encapsulated between the membranes. The passive membrane is made of VHB4905 while the active one is made of VHB4910. When the active membrane is actuated, the in-plane tension is reduced causing a redistribution of the enclosed fluid and a variation of the focal length. The two membranes are modelled with the dynamic model proposed

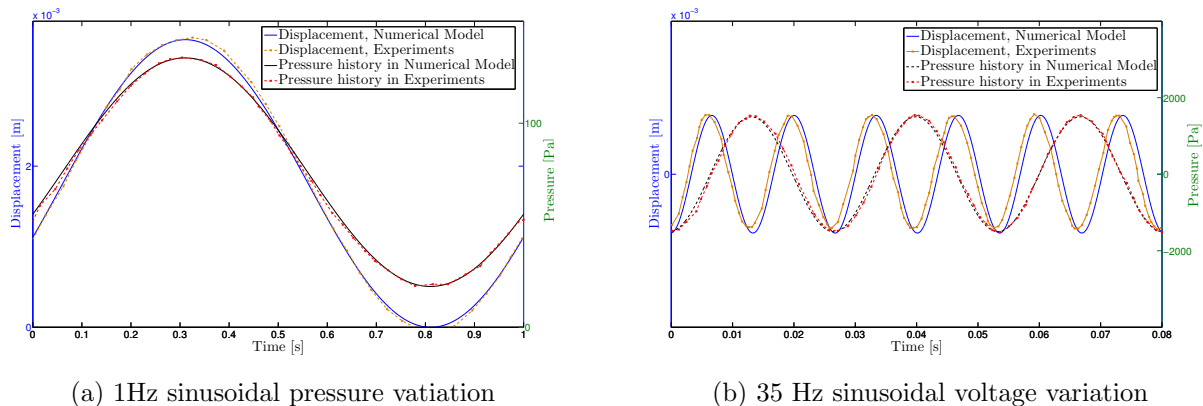


Figure 2: Dynamic actuation of the circular VHB4905 membrane. Experimental data [21] (solid lines) are compared with the numerical models proposed for a) 1Hz sinusoidal pressure and b) 35 Hz sinusoidal voltage.

in Section 3. The Gent model is chosen for the elastic-equilibrium stresses, while the Neo-Hookean one is used for the viscous stresses. The initial selected focal length  $f_0$  is 5.40 mm, with passive and active membranes diameters respectively of  $D_1 = 10$  mm and  $D_2 = 16$  mm and the frame thickness is 4 mm. The passive membrane prestretch is  $\lambda_1 = 2.0$  while the active one is  $\lambda_2 = 4.0$ . The material model considered for the VHB4905 membrane is the one proposed in Section 3.2. The elastic active membrane model is fitted in order to obtain the best agreement with the experimental data given the boundary conditions. The elastic coefficients of the Gent material model used are  $\mu = 24$  kPa and  $J_m = 90$ . The values of the coefficients obtained from the fitting of the static inflation of the VHB4910 membrane proposed by [25] that are found to be close to  $\mu = 22$  kPa and  $J_m = 95$ . The error between the two shear moduli,  $\delta_\mu$ , is less than 10%.

The initial fluid volume and pressure determine the initial focal length. This configuration, identified by the displacements of the passive and active membranes  $z_{10}$  and  $z_{20}$ , is taken as reference configuration for the model and, as in Section 3,  $\Delta z_1$  and  $\Delta z_2$  are the displacements of the passive and active membrane from the reference point. When the active membrane is actuated, the pressure of the fluid is reduced till both the membranes are in equilibrium and the constant volume constraint is satisfied.

A comparison of the static model with experimental data from [4] is presented in Fig. 3b. The performances predicted by the lens model proposed are represented by the black solid line in Fig. 3b. The initial focal length is considered as a constraint and the shear modulus of the active membrane is varied in the range of values determined by the  $\delta_\mu$  error previously defined. The corresponding variation of performance is defined by the dash lines in Fig. 3b. A softer active membrane would lead to higher variations of the focal length. This is due to the greater impact that the applied Maxwell stress will have and to the higher volume of fluid available for displacement [4]. Contrarily, a stiffer active

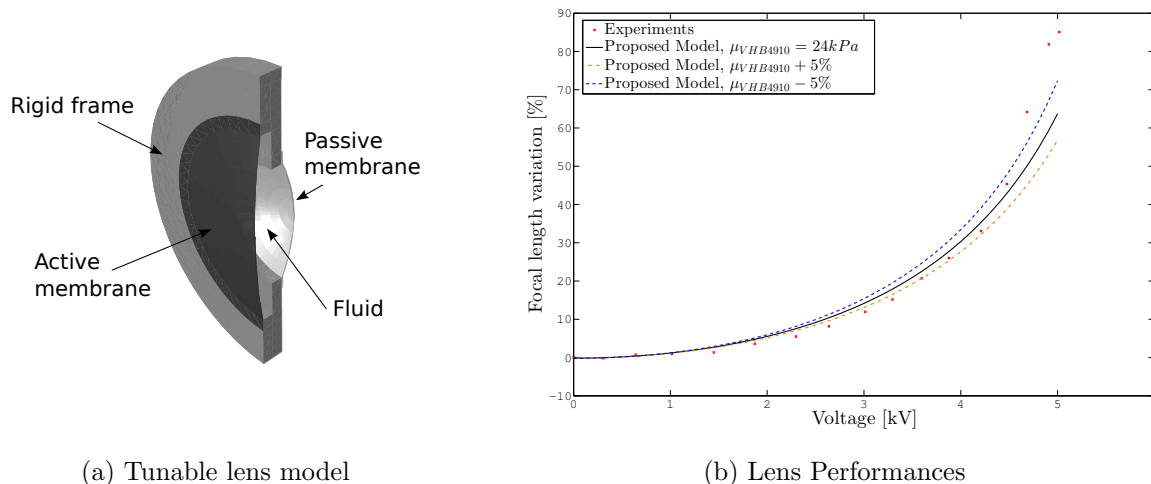


Figure 3: a) Tunable lens model. b) Performances of the actuated lens. Experimental data (symbols) from [4] are compared with the numerical model proposed.

membrane leads to lower performance.

## 5 Conclusions

The design process and performance evaluations of DE actuators require a numerical model able to deal with large deformations, material nonlinearities, viscoelastic effects, and electrostriction. The constitutive model needs to be representative of the effective loading conditions of the actuators and has to include viscoelastic effects to be able to reproduce a wide range of cases. This work proposed a dynamic, non-linear visco-hyperelastic model suitable for finite-element software implementation that can be used for the most common applications of DEs. The coefficients of the model have been defined considering dynamic actuation experiments at various frequencies, with dynamic pressure variation and sinusoidal voltage. The static model showed excellent agreement with experimental data in the literature and it has proven to be predictive for general applications of DEs, as in the case of the tunable lens problem.

## 6 Acknowledgements

The authors would like to acknowledge the financial support of the European Office of Aerospace Research & Development of the US Air Force Office of Scientific Research. This work is funded by the UK Engineering and Physical Sciences Research Council Grant EP/J002070/1, “Towards Biologically-Inspired Active-Compliant-Wing Micro-Air-Vehicles”. This support is gratefully acknowledged.

**REFERENCES**

- [1] A. Tews, K. Pope, and A. Snyder, “Pressure-volume characteristics of dielectric elastomer diaphragms,” in *Smart Structures and Materials 2003: Electroactive Polymer Actuators and Devices (EAPAD)*.
- [2] Y. Bar-Cohen, “Electroactive polymers as artificial muscles - reality and challenges,” 2001.
- [3] F. Carpi, G. Frediani, S. Turco, and D. De Rossi, “Bioinspired tunable lens with muscle-like electroactive elastomers,” *Advanced Functional Materials*, vol. 21, pp. 4152–4158, 2011.
- [4] S. Shian, R. Diebold, and D.R. Clarke, “Tunable lenses using transparent dielectric elastomer actuators,” *Optical Society of America*, vol. 21, pp. 8669–8676, 2010.
- [5] M. Hays, J. Morton, B. Dickinson, K. Uttam, and W. Oates, “Aerodynamic control of micro air vehicle wings using electroactive polymers,” *Journal of Intelligent Material Systems and Structures*, vol. 24, pp. 862–878.
- [6] K. Hochradel, S. Rupitsch, A. Sutor, R. Lerch, D. Vu, and P. Steinmann, “Dynamic performances of dielectric elastomers utilized as acoustic actuators,” *Applied Physics A*, vol. 107, pp. 531–538, 2012.
- [7] Z. Suo, “Theory of dielectric elastomers,” *Acta Mechanica Solida Sinica*, vol. 23, pp. 549–577, 2010.
- [8] J. Fox and N. Goulbourne, “On the dynamic electromechanical loading of dielectric elastomer membranes,” *Journal of the Mechanics and Physics of Solids*, vol. 56, pp. 2669–268, 2008.
- [9] M. Wissler and E. Mazza, “Electromechanical coupling in dielectric elastomer actuators,” *Sensors and Actuators A: Physical*, vol. 138, pp. 384–393, 2007.
- [10] T. Li, C. Keplinger, R. Baumgartner, S. Bauer, W. Yang, and Z. Suo, “Giant voltage-induced deformation in dielectric elastomers near the verge of snap-through instability,” *Journal of the Mechanics and Physics of Solids*, vol. 61, pp. 611–628, 2013.
- [11] H. Mokarram, D. Vu, and P. Steinmann, “Experimental study and numerical modelling of vhb 4910 polymer,” *Computational Materials Science*, vol. 59, pp. 65–74, 2012.
- [12] J. Bonet, “Large strain viscoelastic constitutive models,” *International Journal of Solids and Structures*, vol. 38, 2001.

- [13] A. Schmidt, A. Bergamini, G. Kovacs, and E. Mazza, “Multi-axial mechanical characterization of interpenetrating polymer network reinforced acrylic elastomer,” *Experimental Mechanics*, vol. 51, pp. 1421–1433, 2011.
- [14] J. Simo and T. Hughes, *Computational Inelasticity*. Springer: Interdisciplinary applied mathematics: Mechanics and materials, 1998.
- [15] V. Tagarielli, R. Hildick-Smith, and J. Huber, “Electro-mechanical properties and electrostriction response of a rubbery polymer for eap applications,” *International Journal of Solids and Structures*, vol. 49, pp. 3409–3415, 2012.
- [16] X. Zhao and Z. Suo, “Electrostriction in elastic dielectrics undergoing large deformation,” *Journal of Applied Physics*, vol. 104, 2008.
- [17] J. Bonet and R. Wood., *Nonlinear continuum mechanics for finite element analysis*. Cambridge, UK: Cambridge University Press, 2008.
- [18] P. Flory, “Thermodynamic relations for high elastic materials,” *Transactions of the Faraday Society*, vol. 57, pp. 829–838, 1961.
- [19] M. Wissler and E. Mazza, “Modeling of a pre-strained circular actuator made of dielectric elastomers,” *Sensors and Actuators A: Physical*, vol. 120, pp. 184–192, 2005.
- [20] M. Wissler and E. Mazza, “Modeling and simulation of dielectric elastomer actuators,” *Smart Materials and Structures*, vol. 14, pp. 1396–1402, 2005.
- [21] J. Fox and N. Goulbourne, “Electric field-induced surface transformations and experimental dynamic characteristics of dielectric elastomer membranes,” *Journal of the Mechanics and Physics of Solids*, vol. 57, pp. 1417–1435, 2009.
- [22] S. Son and N. Goulbourne, “Dynamic response of tubular dielectric elastomer transducers,” *International Journal of Solids and Structures*, vol. 47, pp. 2672–2679, 2010.
- [23] C. Suchocki, “A finite element implementation of knowles stored-energy function: theory, coding and applications,” *The Archive of mechanical engineering*, vol. LVIII, pp. 319–346, 2011.
- [24] A. Gent, “A new constitutive relation for rubber,” *Rubber Chemistry Technology*, vol. 69, 1996.
- [25] J. Fox, “Electromechanical characterization of the static and dynamic response of dielectric elastomer membranes,” Master’s thesis, Master thesis, Virginia Polytechnic Institute and State University., 2007.